Original Article

A Fuzzy Cognitive Map-based Framework for Alzheimer's Disease Diagnosis Using Multimodal Magnetic Resonance Imaging-Positron Emission Tomography Registration

Seyed Assef Mahdavi[1], Keivan Maghooli[2], Fardad Farokhi[1]

[1]Department of Biomedical Engineering, Central Tehran Branch, Islamic Azad University, Tehran, Iran, [2]Department of Biomedical Engineering, Science and Research Branch, Islamic Azad University, Tehran, Iran

Abstract

Background: Alzheimer's disease (AD) is a progressive and irreversible brain disorder, characterized by a gradual decline in cognitive and memory function, with memory loss being one of the most prominent symptoms. Accurate and early diagnosis of AD is essential for effective management and treatment. Structural magnetic resonance imaging (sMRI) and positron emission tomography (PET) are widely utilized neuroimaging modalities for diagnosing AD due to their ability to provide complementary structural and functional insights into brain abnormalities. **Methods:** This study introduces a novel computer-aided diagnosis system that integrates sMRI and PET data using Fuzzy Cognitive Maps (FCM) to improve diagnostic accuracy. The research is conducted using the ADNI dataset, where preprocessing of sMRI and PET images is performed using FSL and statistical parametric mapping tools, respectively. In a key innovation, features extracted from both modalities are fused and dimensionality reduction is achieved through an Autoencoder model. The reduced feature set is then classified using FCM, Support Vector Machine, k-Nearest Neighbors, and Multilayer Perceptron. **Results:** The FCM-based approach demonstrates superior performance, achieving the highest accuracy of 93.71%, surpassing other classifiers tested. **Conclusions:** This study underscores the effectiveness of integrating FCM with multimodal neuroimaging data and highlights its potential for enhancing the early and reliable diagnosis of AD.

Keywords: *Alzheimer disease, autoencoder, diagnosis, fuzzy cognitive maps, magnetic resonance imaging-positron emission tomography*

Submitted: 07-Jan-2025 **Revised:** 08-Mar-2025 **Accepted:** 26-May-2025 **Published:** 01-Nov-2025

Introduction

Alzheimer's disease (AD) progressively affects the millions of people worldwide, causing a gradual decline in cognitive and memory functions. Many individuals experience memory loss as one of the earliest and most prominent symptoms, which significantly disrupts their daily activities. People often misattribute these early symptoms to stress or the natural aging process, which delays timely diagnosis and intervention.[1] Neuropsychological tests, such as the Mini-Mental State Examination (MMSE) and the Mini-Cog Test, can detect mild cognitive impairment (MCI) up to 8 years before clinical diagnosis.[2-4] However, these assessments alone are insufficient for definitive AD diagnosis and need to be complemented by neuroimaging and clinical evaluations.[1,5,6]

AD typically progresses through three stages: early (mild), middle (moderate), and late (severe).[4,7] The hippocampus, a critical region for memory and learning, is particularly vulnerable to AD-related damage, leading to atrophy in the regions such as the temporal lobe and the cingulate cortex.[8,9] This neuronal loss underscores the importance of neuroimaging techniques for detecting structural and functional brain changes associated with AD.

Neuroimaging modalities, including structural magnetic resonance imaging (sMRI) and Positron Emission Tomography (PET), are widely used for AD diagnosis.[10-12] sMRI provides detailed structural information, highlighting brain atrophy and tissue changes, while PET captures functional and metabolic alterations through radiotracers.[13,14] The combination of these modalities offers a comprehensive view of the brain, enhancing

How to cite this article: Mahdavi SA, Maghooli K, Farokhi F. A fuzzy cognitive map-based framework for Alzheimer's disease diagnosis using multimodal magnetic resonance imaging-positron emission tomography registration. J Med Sign Sens 2025;15:31.

Address for correspondence:
Dr. Keivan Maghooli, Department of Biomedical Engineering, Central Tehran Branch, Islamic Azad University, Tehran, Iran.
E-mail: k_maghooli@srbiau.ac.ir

Access this article online

Website: www.jmssjournal.net

DOI: 10.4103/jmss.jmss_3_25

Quick Response Code:

diagnostic accuracy.[15,16] Advances in machine learning (ML) have further improved the analysis of neuroimaging data, enabling the detection of subtle patterns that may elude human observation. ML algorithms can process large datasets, identify diagnostic biomarkers, and reduce the subjectivity inherent in traditional diagnostic methods, leading to more standardized and reproducible diagnoses.[1-3]

This study introduces a ML-based computer-aided diagnosis (CAD) system that leverages multimodal sMRI and PET data for the diagnosis of AD. The CAD system follows a five-step process: dataset selection, preprocessing, feature extraction, feature reduction, and classification. The ADNI dataset, comprising data from both AD patients and HC, was used for the experiments. Preprocessing was conducted using FMRIB software library (FSL) and statistical parametric mapping (SPM) tools to ensure high-quality input data. Feature extraction from sMRI and PET images was followed by dimensionality reduction using an Autoencoder (AE). The reduced features were then classified using multiple methods, including fuzzy cognitive maps (FCM), support vector machine (SVM), k-Nearest neighbors (KNNs), and multilayer perceptron (MLP).

Therefore, the true novelty of our work lies in the synergistic integration of AE for feature extraction, FCM for classification, and MRI-PET fusion within a single optimized framework, which has not been extensively explored in previous AD diagnosis studies. The key contributions of this work are as follows:

1. Innovative Feature Fusion and Dimensionality Reduction: While AE have been previously used for feature reduction, our approach uniquely employs AE to fuse multimodal MRI and PET data, ensuring that the most discriminative features are preserved while reducing redundancy
2. Hybrid Classification Model with FCM: Although FCM has been used for classification in other domains, its application within a hybrid classification pipeline alongside SVM, KNN, and MLP enhances decision-making robustness and model interpretability
3. Comprehensive Multimodal Integration: Unlike previous studies that use independent structural (sMRI) or functional (PET) data, this study optimally combines MRI and PET at the feature level using AE-based integration and applies a multi-classifier strategy for AD detection, improving diagnostic accuracy.

This study establishes a new benchmark for multimodal neuroimaging-based AD diagnosis. The proposed methodology improves both accuracy and interpretability, making it a promising approach for clinical decision support systems.

The remainder of this paper is structured as follows: Section 2 reviews related work on AD diagnosis using multimodal MRI-PET and ML techniques. Section 3 details the proposed CAD system, including dataset selection, preprocessing, feature extraction, feature reduction, and classification. Section 4 presents the experimental results and Section 5 discusses the findings, study limitations, and directions for future research.

Related works

Numerous studies have applied ML and DL techniques for AD diagnosis using multimodal MRI-PET data. These studies generally involve preprocessing steps such as normalization, segmentation, and feature extraction to enhance data quality. For classification, methods such as SVM, MLP, and FCM have been widely used. Researchers such as Tabarestani *et al*.[17] and Ding and Huang[18] successfully employed SVM after feature extraction and selection. Krashenyi *et al*.[19] used the FCM method, while Polikar *et al*.[16] applied ensemble learning techniques with wavelet-based features. Additionally, methods like BP and RF have also shown promising results in various studies.[20,21]

Overall, these studies demonstrate that integrating MRI and PET data, combined with advanced AI techniques, improves the accuracy and efficiency of AD diagnosis, providing valuable tools for clinical applications.

Table 1 summarizes the key studies on AD diagnosis using MRI-PET data, detailing their methodologies and approaches. The number of subjects varies significantly across studies, ranging from small datasets with 20–50 subjects to larger datasets with over 1000 subjects. Most studies employ preprocessing steps such as normalization, segmentation, and registration to standardize the data. Feature extraction techniques differ widely, including voxel intensity, cortical thickness, and atlas-based methods (e.g., Individual brain atlases using SPM Atlas or Automated Anatomical Labeling [AAL] atlas). For feature selection, methods such as the L1 norm, Laplace eigenmaps, and the *t*-test are commonly used to reduce dimensionality.[17]

In the classification phase, methods such as SVM, MLP, and FCM are applied. For instance, Tabarestani *et al*.[17] utilized MLP and SVM, while Krashenyi *et al*.[19] implemented the FCM method for clustering and classification. Studies such as Ding and Huang[18] focused on SVM for classifying cortical thickness and voxel features. Overall, SVM appears to be the most frequently used classifier, reflecting its effectiveness in handling high-dimensional neuroimaging data. These studies highlight the importance of integrating preprocessing, feature extraction, and robust classification techniques to improve AD diagnosis accuracy. Sheng *et al*.[22] proposed a hybrid ML model incorporating MRI, PET, and cerebrospinal fluid (CSF) biomarkers, where the ILHHO-KELM algorithm significantly outperformed single-modality approaches, achieving a classification accuracy of 99.2% on the ADNI dataset. Similarly, Tang *et al*.[23] leveraged a three-dimensional (3D) convolutional neural network (CNN) and transformer model to capture

Table 1: Related works in the diagnosis of Alzheimer's disease from magnetic resonance imaging and positron emission tomography modalities

References	Number of subjects	Preprocessing	Feature extraction	Feature selection	Classification
[17]	333 AD patients, 529 LMCI, 255 EMCI, 341 HC	Normalization	38 features	L1 norm	MLP, SVM
[18]	Different subjects	Cortex segmentation and reconstruction, presmoothing Realignment, registration, normalization, SUVr, AAL	Cortical thickness, voxel features	Laplace Eigen maps of images	SVM
[19]	70 AD, 111 MCI, 68 HC	Normalization, segmentation, voxel selection procedure Normalization	IBASPM atlas, mean values of voxel intensities over the whole ROI	t-test	FCM
[27]	28 AD, 28 HC 21 AD, 13 HC	Different methods	VOI extraction, mean value of each VOI	-	SVM
[28]	45 AD, 50 HC	Hybrid FCM/PCM brain image segmentation	-	-	SVM
[29]	70 AD, 214 EMCI, 103 LMCI, 137 HC	Free surfer	Different features 15 significant PET uptake features (7 for FDG and 8 for Av-45)	-	OPLS analysis
[30]	20 AD, 18 HC	Masking	219727 voxels	-	SVM

AD – Alzheimer's disease; PET – Positron emission tomography; SVM – Support vector machine; FCM – Fuzzy cognitive maps; ROI – Region of interest; AAL – Automated anatomical labeling; VOI – Volumes of interest; IBASPM – Individual brain atlases using statistical parametric mapping; MCI – Mild cognitive impairment; LMCI – Late MCI; EMCI – Early MCI; PCM – Possibilistic C-means; OPLS – Orthogonal partial least squares; HC – Healthy control, SUVr – Standardized uptake value ratio

spatial and contextual relationships in MRI-PET data, identifying the left parahippocampal region as a key area associated with AD.

The importance of 3D neuroimaging was highlighted by Castellano *et al*.,[24] who demonstrated that integrating 3D MRI and amyloid PET scans improved classification accuracy, achieving state-of-the-art performance on the OASIS-3 dataset. Generative models have also been explored for AD diagnosis. Choudhury *et al*.[25] developed a coupled-GAN (CGAN) architecture to fuse MRI and PET features, significantly improving the classification of MCI to AD. Zhang *et al*.[26] proposed a multi-modal graph neural network, incorporating imaging and phenotypic data to enhance early diagnosis, demonstrating superior performance over single-modality approaches.

Materials and Methods

This section introduces the proposed CAD system for diagnosing AD using MRI-PET data. Figure 1 illustrates the method block diagram.

Dataset

For the experiments conducted in this study, we used the AD Neuroimaging Initiative (ADNI) dataset, a widely recognized resource for neuroimaging research on AD. The ADNI dataset includes comprehensive medical imaging data, clinical assessments, genetic information, and biospecimens collected from multiple subjects. For our research, we focused specifically on subjects who had both MRI and PET modalities available.

We selected subjects diagnosed with AD and HC to ensure a balanced comparison. After filtering the dataset to include only cases where both MRI and PET data were available for the same individuals, the final dataset consisted of 61 AD patients and 58 HC subjects, totaling 119 subjects.

For our research, we conducted all experiments using FDG-PET and T1-weighted MRI data from 119 subjects. It is important to note that only subjects with both PET and MRI modalities, as available in the ADNI data, were included in our tests. The age range of the HC and AD data was 75.81 ± 4.93 and 75.33 ± 7.17, respectively. In this work, we use the raw ADNI data. The next section will outline the preprocessing steps we took to prepare the data for our analysis.

In this study, we used a trial-and-error approach for parameter tuning on the train-set. At no point were test-set labels or results used for tuning to ensure a fair and unbiased evaluation of model performance. The parameters were iteratively adjusted based on performance metrics obtained from the train-set, and the final configuration was selected based on the best validation performance.

Preprocessing

This section discusses the preprocessing techniques applied to sMRI and PET data for diagnosing brain diseases using neuroimaging modalities. Accurate disease diagnosis critically depends on effective preprocessing methods. The first step involves normalizing the sMRI and PET data to ensure each voxel in the image

corresponds accurately to its anatomical location. The MRI images were normalized to the MNI152 template using the FSL pipeline, while PET images underwent intensity normalization and spatial realignment using SPM. Co-registration was performed to align PET images with corresponding MRI scans, ensuring consistency in feature extraction across modalities. In addition, stratified train-test splitting was used to ensure a balanced representation of classes. While some degree of overfitting may still occur, our model selection and validation approach helped improve generalizability. The following subsections provide detailed explanations of the specific preprocessing steps used for sMRI and PET data.

Structural magnetic resonance imaging preprocessing

The preprocessing of sMRI data involved several key steps to ensure consistency and quality across all scans. The sMRI images in the ADNI dataset were acquired in three anatomical planes: sagittal, coronal, and axial views. During the image registration process, we standardized and resized the images, ensuring uniform dimensions and alignment. The slice thickness for these MRI scans was set to 1.5 mm, providing high-resolution detail necessary for detecting structural brain changes related to AD. We utilized the FSL toolbox for segmenting the MRI images into three primary tissue types: white matter (WM), gray matter (GM), and CSF. Since GM regions are most affected in AD and provide crucial information about neurodegeneration, we focused on GM for subsequent analysis and feature extraction.

Figure 2 illustrates the examples of the preprocessed sMRI images for both AD patients and HC, showcasing the segmented GM regions. These preprocessing steps – standardization, registration, and segmentation – ensured high-quality data, optimized for accurate feature extraction and classification in later stages of the study.

Positron emission tomography preprocessing

We employed SPM tools to preprocess the PET data, following a series of essential steps to ensure consistency and quality for accurate AD diagnosis. The PET images were standardized to a slice thickness of 3 mm. To ensure comparability across scans, we applied intensity normalization, which adjusts the intensity levels of each image to a standard reference.

For normalization, we used the mean image method, where the normalization value for each image was calculated as the mean intensity of the top 1% of voxels with the highest activation levels in the template. This normalization step is critical for achieving consistent intensity levels and enhancing the reliability of subsequent analyses and comparisons.

We further processed the PET data using the AAL atlas[31] to define and extract the specific regions of interest (ROIs). The AAL atlas initially provided 108 regions, but based on previous research, we focused on 42 regions located in the frontal, parietal, occipital, and temporal lobes, which are particularly relevant for diagnosing AD.[32] Extracting these specific regions enhances the efficiency and accuracy of the diagnostic process.

Table 2 lists the 42 critical regions extracted from the PET data and Figure 3 presents the examples of preprocessed PET images. These preprocessing steps – intensity normalization, ROI extraction, and standardization – play a pivotal role in ensuring the PET data is ready for feature extraction and subsequent classification.

Feature extraction

Feature extraction from sMRI and PET data plays a critical role in the diagnosis of AD. For sMRI images, we selected

Table 2: Important regions of interest s for diagnosis of Alzheimer's disease from positron emission tomography modality

Frontal	Partial	Occipital	Temporal
Frontal_Sup_L	Parietal_Sup_L	Occipital_Sup_L	Temporal_Sup_L
Frontal_Sup_R	Parietal_Sup_R	Occipital_Sup_R	Temporal_Sup_R
Frontal_Mid_L	Parietal_Inf_L	Occipital_Mid_L	Temporal_Pole_Sup_L
Frontal_Mid_R	Parietal_Inf_R	Occipital_Mid_R	Temporal_Pole_Sup_R
Frontal_Sup_Medial_L	Precuneus_L	Occipital_Inf_L	Temporal_Mid_L
Frontal_Sup_Medial_R	Precuneus_R	Occipital_Inf_R	Temporal_Mid_R
Frontal_Mid_Orb_L	Cingulum_Post_L		Temporal_Pole_Mid_L
Frontal_Mid_Orb_R	Cingulum_Post_R		Temporal_Pole_Mid_R
Rectus_L			Temporal_Inf_L 8301
Rectus_R			Temporal_Inf_R 8302
Cingulum_Ant_L			Fusiform_L
Cingulum_Ant_R			Fusiform_R
			Hippocampus_L
			Hippocampus_R
			ParaHippocampal_L
			ParaHippocampal_R

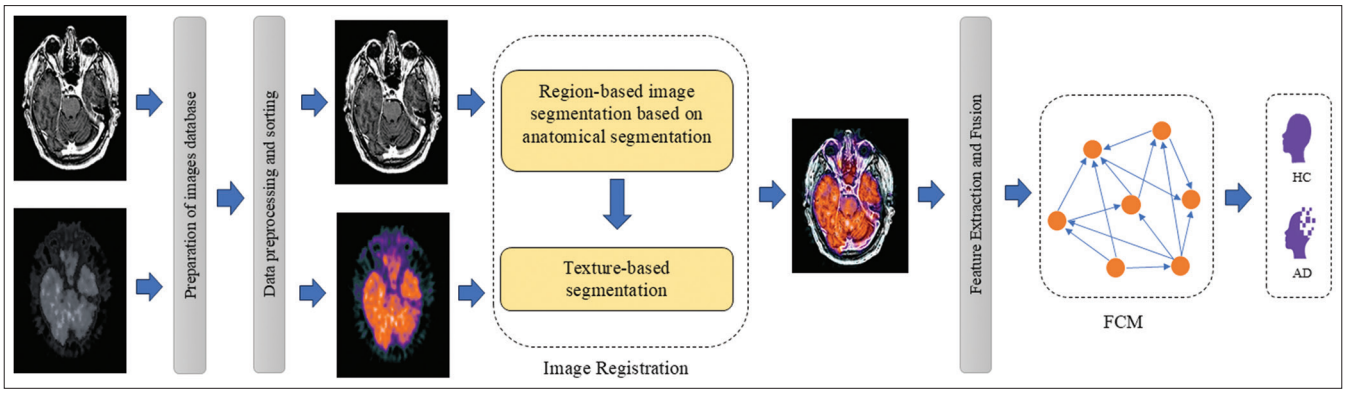

Figure 1: Method block diagram. FCM – Fuzzy cognitive maps

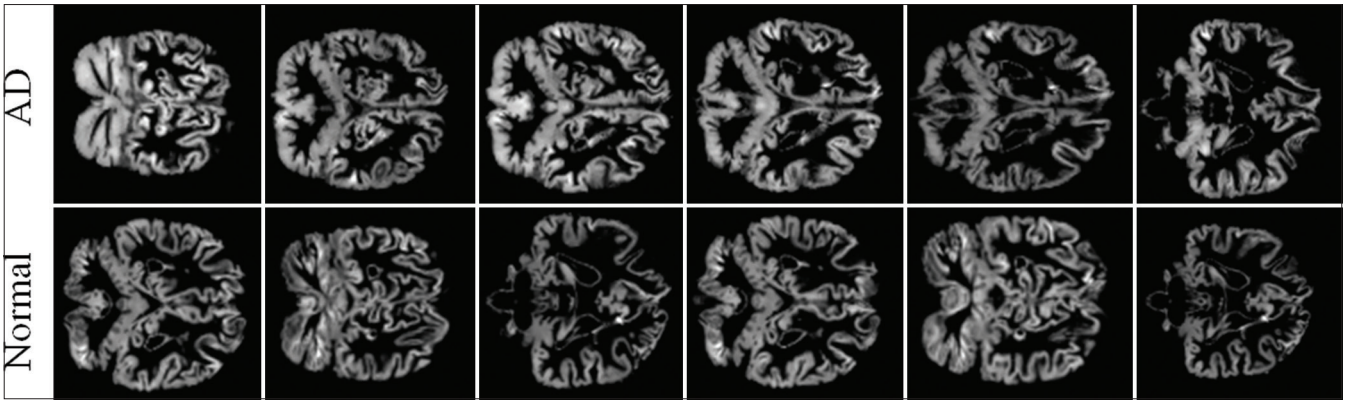

Figure 2: Structural magnetic resonance imaging (MRI) scans of Alzheimer's disease (AD) patients and normal controls after preprocessing using the FSL toolbox

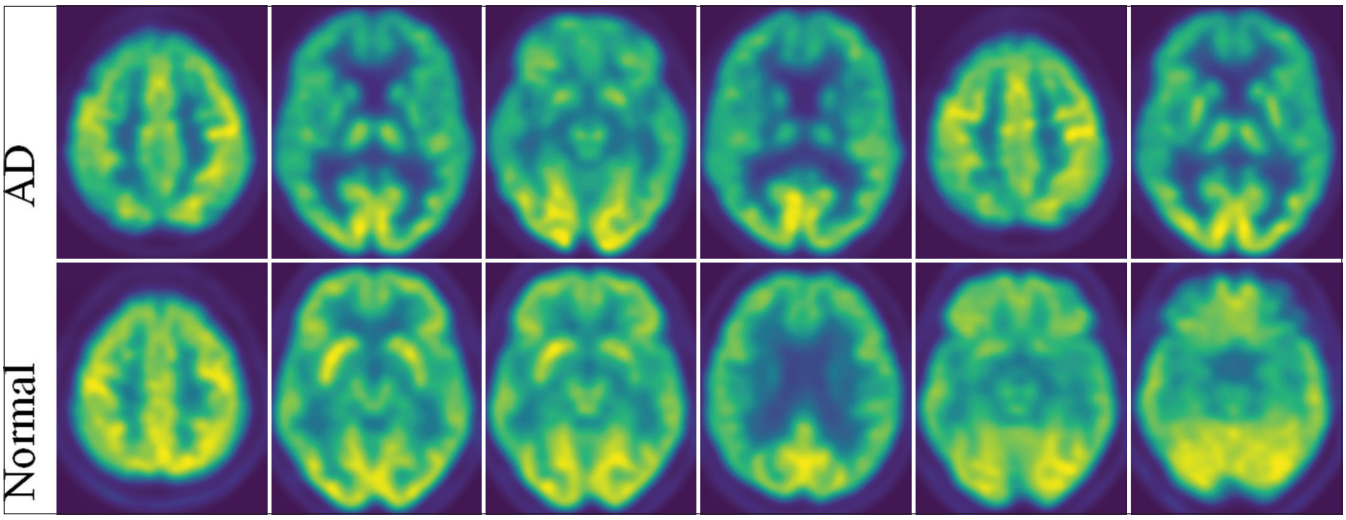

Figure 3: Positron emission tomography (PET) scans of Alzheimer's disease (AD) patients and normal controls after preprocessing

60 high-quality images per subject, captured in sagittal, coronal, and axial views. The selection of 60 high-quality images per subject was based on a combination of objective criteria and visual assessment. First, images were chosen based on signal-to-noise ratio (SNR) and contrast-to-noise ratio (CNR) to ensure clarity and minimal artifacts. Second, images with excessive motion artifacts or intensity distortions were excluded. Third, anatomical completeness was assessed to ensure that the relevant brain structures were clearly visible. A minimum threshold for SNR and CNR was applied to standardize the selection process, ensuring consistency across all subjects.

In addition, we employed texture-based methods like the Gray Level Co-occurrence Matrix (GLCM) and Gray Level Run Length Matrix (GLRLMS) to capture spatial

information. GLCM was chosen for its ability to assess spatial dependencies and texture variations indicative of neurodegeneration, with extracted features including energy, contrast, correlation, entropy, and difference variance.

GLRLMS was selected for its capability to characterize structural heterogeneity, providing measures such as short-run emphasis, long-run emphasis, gray-level nonuniformity, and high gray-level run emphasis. These features are essential for identifying subtle changes in brain tissue associated with AD.

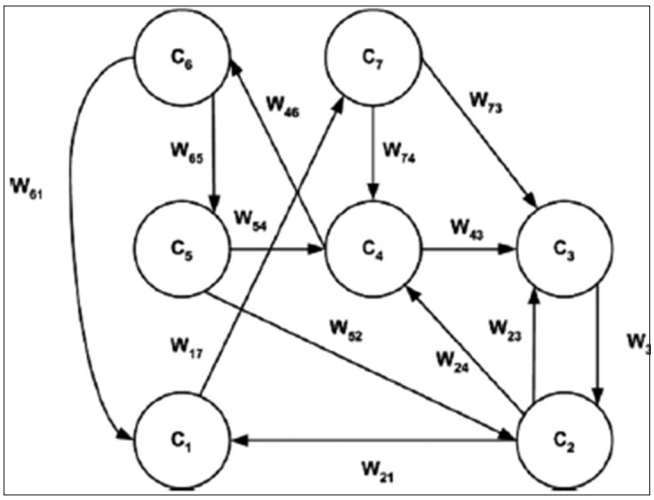

Figure 4: Graphs in fuzzy cognitive map

For PET images, we applied multiple texture analysis methods, including Gray Level Histogram Analysis (GLHA), GLCM, Neighborhood Gray Tone Difference Matrix (NGTDM), and Gray Level Size Zone Matrix (GLSZM). GLHA was used to quantify intensity distribution variations, capturing important metabolic changes. These methods extracted 27 features per region of interest (ROI), including mean, variance, skewness, contrast, dissimilarity, entropy, and homogeneity. NGTDM was chosen for its ability to highlight local intensity variations, extracting features such as busyness, coarseness, and complexity, while GLSZM was utilized to assess spatial heterogeneity through features like intensity variability, small area emphasis, and zone percentage. By carefully selecting and fusing the extracted features from both sMRI and PET modalities, we ensured a comprehensive feature representation that enhances the accuracy and robustness of AD diagnosis.

To assess the effectiveness of the AE in feature selection, we compared it with principal component analysis (PCA) and recursive feature elimination (RFE), two widely used dimensionality reduction methods. PCA is effective for reducing feature dimensionality by transforming data into orthogonal components; however, it relies on linear

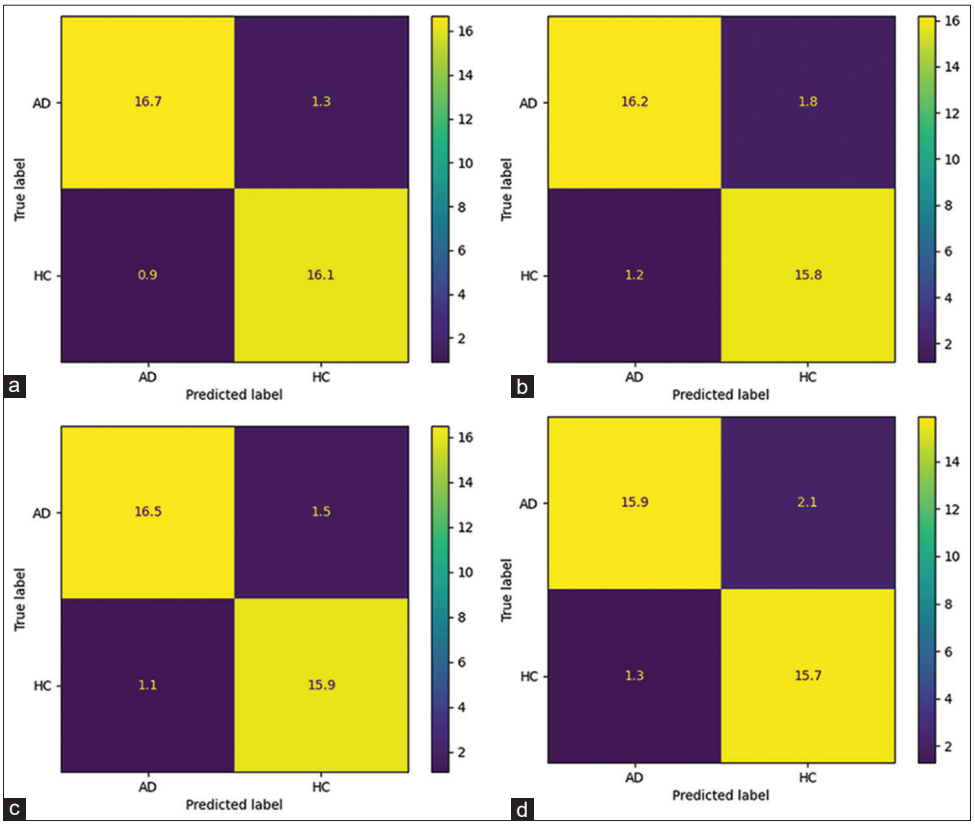

Figure 5: Confusion matrix for fuzzy cognitive maps (FCM) (a), Multilayer perceptron (b), Support vector machine (c), and k-Nearest Neighbor (d). AD – Alzheimer's disease

transformations and may fail to capture the complex nonlinear relationships in neuroimaging data. RFE, on the other hand, systematically removes less important features based on model performance but requires extensive computational resources to identify optimal feature subsets. In contrast, AE efficiently preserved critical nonlinear feature representations while achieving substantial dimensionality reduction. Given its superior ability to retain essential multimodal information, AE was selected as the feature selection method for this study.

Feature selection

Feature reduction using AI techniques is a crucial step in CADS. The primary objective of feature reduction or feature selection is to employ essential features as input for classification algorithms to accurately diagnose a disease. This, in turn, enhances the speed and efficiency of classification algorithms. Various techniques have been proposed to reduce the dimensionality of the feature matrix, which can be categorized as ML and DL techniques. In this study, an AE was proposed to reduce features. AE models are based on unsupervised learning and used for various purposes, including feature selection. Unlike conventional techniques like PCA, AE has higher performance in terms of feature reduction.[33] We conducted extensive experimentation to optimize the hyperparameters of the AE for feature selection. The final configuration was chosen based on its ability to achieve optimal dimensionality reduction while preserving key features relevant to AD diagnosis. The selection process involved iterative experimentation with different architectures, where each configuration was evaluated using reconstruction error and classification accuracy metrics. The learning rate, activation function, and optimizer were fine-tuned to balance convergence speed and performance. We monitored loss curves over multiple training epochs to prevent overfitting and ensured that the latent space representation retained discriminative information. The finalized AE model, along with its hyperparameters, is summarized in Table 3.

Classification

Fuzzy cognitive map

A FCM is a directed graph with feedback and signed edges. Introduced by Kosko in 1986, FCMs are a method for modeling complex systems by describing the causal relationships among the primary factors (concepts) and determining the dynamic behavior of a system.[34]

FCMs are graphically represented by nodes with interconnections between them. As illustrated in Figure 4, an FCM consists of nodes called concepts, denoted by Ci, with i = 1, 2, 3., N, where N is the total number of concepts that represent the characteristics, main factors, or properties of the system being modeled. The concepts are connected by weighted arcs that represent the causal relationships between them. The direction of these edges was determined based on a combination of expert knowledge and statistical analysis of feature dependencies. Initially, domain experts established a preliminary graph structure based on known interactions in AD progression. Three types of causal relationships can be identified between two concepts Ci and Cj: positive causality (wij > 0), negative causality (wij < 0), and absence of relation (wij = 0). Positive causality indicates that an increase (decrement) in the value of a cause concept leads to movement of the effect concept in the same direction and is represented by a positive weight (wij). Conversely, negative causality suggests that the changes in the cause-and-effect concepts are in the opposite direction, and the weight (wij) has a negative sign. When there is no relation between the concepts, the weight wij equals zero. The value of wij indicates the strength of the influence of concept Ci on concept Cj, and it takes values in the fuzzy causal interval (−1, 1).

In determining the value, Ai, of each concept Ci, the effects of all other concepts are aggregated, and the overall effect is transformed using the barrier function f, according to the following rule.[34]

$$A_i^{(t+1)} = f(A_i^{(t)} + \sum_{(i=1,\, j \neq i)}^{N} W_{ji} A_j^{(t)})$$

Where, $A_i^{(t+1)}$ and $A_i^{(t)}$ are the values of concept Ci at

Table 3: Hyper-parameters for the proposed autoencoder model

Hyperparameter	Value	Description
Number of layers	6	Ensures optimal depth for feature extraction
Neurons per layer	1024, 512, 256, 128, 256, 512	Gradual reduction and reconstruction of features
Activation function	ReLU	Provides nonlinearity for better feature learning
Latent dimension	128	Compressed representation of original features
Optimizer	Adam	Adaptive optimization for efficient training
Learning rate	0.001	Controls the step size during training
Loss function	MSE	Measures reconstruction error
Batch size	32	Determines the number of samples per training iteration
Training epochs	50	Ensures sufficient learning while preventing overfitting
Dropout rate	0.2	Prevents overfitting by randomly dropping connections
Weight initialization	Xavier initialization	Ensures balanced weight distribution

MSE – Mean squared error

times $t + 1$ and t, respectively. $A_j^{(t)}$ is the value of the concept Cj at time t. W_{ji} represents the weight value of the interconnection directed from concept Cj to concept Ci, while f is a barrier function that constrains the value of the concept within a specified range, such as (1, 0) or (1, −1).

Using equation (1), a new state of concepts is determined at each step, and after several iterations, the FCM can attain one of the following states: (1) a fixed equilibrium point, (2) a limit cycle, or (3) a chaotic behavior. When the FCM reaches a fixed equilibrium point, it is considered to have converged, and the final state corresponds to the state of the actual system when the initial values of the concepts are applied.

FCMs are typically designed based on prior knowledge and experience with the system being modeled to determine the weight values for the interconnections between concepts. In more flexible FCM structures, these weights can be learned through a training procedure, similar to neural network training. As a result, researchers have adopted and adapted algorithms from the neural network theory to develop new learning methods. In this study, the Hebbian training method was employed for the FCM technique.[34] The Hebbian learning method used in our FCM model updates connection weights based on co-occurrence patterns of concept activations. Specifically, the weight update follows a rule where an increase in one concept's activation leads to a proportional increase or decrease in another, depending on the sign of their relationship. This method simulates learning mechanisms in biological neural networks and enables adaptive updates to the FCM structure.

Support vector machine

SVMs represent a crucial class of ML techniques that are widely employed for various tasks such as classification, regression, and outlier detection. In classification applications, SVMs aim to identify the hyperplane that maximizes the margin between two classes.[35] These models have a strong theoretical foundation and exhibit remarkable accuracy when it comes to separating both linear and nonlinear data. Unlike other models, SVMs prioritize the optimization of the margin over fitting the data, which makes them less susceptible to overfitting. There are different types of SVMs, such as linear SVM, non-linear SVM (NLSVM), multiclass SVM, probabilistic SVM, and regression SVM. The choice of which SVM to apply depends on the nature of the data at hand. For this particular paper, the NLSVM with a Gaussian kernel was utilized.

K-nearest neighbor

KNN is a simple yet effective classification algorithm used for a wide range of classification and regression tasks. Unlike other classification algorithms, KNN does not require a training phase. Instead, it stores all training samples and classifies new samples based on their proximity to the nearest neighbors in the training set.[36] This approach is easy to implement and can be summarized as follows: (1) selection of a K value, (2) calculation of the distance between the new sample and all training samples, (3) selection of K samples with the smallest distance to the new sample, and (4) assigning the new sample class to the class that appears most frequently among the KNN.[36] In this work, the KNN algorithm is implemented for various values of K. Among the tested K values, $K = 3$ proved to be the most successful.

Multilayer perceptron

MLP is a type of neural network that is commonly used for data classification tasks. It consists of multiple layers of interconnected nodes that process the input data and produce an output. The input layer receives the data, the hidden layers perform computations on the input, and the output layer produces the final classification result. One advantage of MLP is its ability to learn complex non-linear relationships between input and output data, making it suitable for a wide range of classification tasks.[37] Additionally, MLP can handle high-dimensional data and can be trained using various optimization algorithms. However, one disadvantage of MLP is that it can be prone to overfitting, where the model learns the training data too well and performs poorly on new, unseen data.[37]

Experimental Results

For the implementation of the proposed method, we used a PC equipped with a Core i7 CPU, 16 GB RAM, and an NVIDIA 1070 GPU. The preprocessing of sMRI data was carried out using the FSL toolbox, while SPM was employed for preprocessing PET data. We performed feature extraction, feature selection, and classification using MATLAB 2021b, TensorFlow 2, and the Scikit-learn library, respectively.

The experiments used the ADNI dataset, which includes MRI and PET scans from subjects diagnosed with AD and HC. We selected subjects for whom both sMRI and PET modalities were available, resulting in a dataset of 61 AD patients and 58 HC subjects. For each subject, we chose 60 high-quality sMRI images and a corresponding PET scan. These images underwent preprocessing to enhance the data quality and standardize inputs for the proposed CAD system. The sMRI data were segmented into WM, GM, and CSF using the FSL toolbox. Since GM regions provide the most relevant information for diagnosing AD, we used these regions for further analysis. For PET data, we employed the AAL atlas to extract 42 ROIs known to be critical for AD diagnosis.

During the feature extraction stage, we extracted 108 unique features from each sMRI image, leading to a total of 108 × 60 features per subject. For PET data, we extracted 27 features per ROI from the 42 selected ROIs, resulting in 27 × 42 features per subject. We combined these features

to form a comprehensive feature vector, yielding 7,797,660 features for each subject. To handle this high-dimensional data, we used an AE model with six layers to reduce the feature set to 32 dimensions. This approach marked the first use of AE-based feature reduction for AD diagnosis in a multimodal MRI-PET framework.

Table 4 highlights the comparative effectiveness of different dimensionality reduction methods. As a linear transformation method, PCA effectively reduced the feature space but struggled to capture complex nonlinear patterns in the multimodal data. This limitation is reflected in its relatively lower classification performance. RFE, which eliminates less relevant features iteratively, performed better than PCA but was computationally expensive and less effective in retaining critical information. In contrast, AE demonstrated superior performance by preserving intricate nonlinear relationships while achieving higher accuracy, precision, recall, and F1-score. These findings confirm that AE is a more suitable feature selection method for multimodal MRI-PET data fusion in AD diagnosis. The improved classification accuracy achieved with AE further supports its effectiveness in handling high-dimensional neuroimaging data and underscores its advantages over conventional techniques.

For classification, we tested multiple ML methods, including FCM, MLP, SVM, and KNN. We implemented the FCM method in Python and used Scikit-learn for the other classifiers. Table 5 presents the performance metrics – accuracy, precision, recall, and F1-Score – for each classifier. The FCM method achieved the highest accuracy of 93.71%, demonstrating superior performance compared to the other methods.

Table 4: Performance comparison of dimensionality reduction methods

Method	Accuracy (%)	Precision (%)	Recall (%)	F1-score (%)
PCA	88.52±0.85	87.89±0.92	89.02±0.76	88.43±0.81
RFE	90.11±0.73	89.32±0.88	90.54±0.81	89.91±0.79
AE (proposed)	93.71±0.72	92.79±0.59	94.70±0.53	93.62±0.60

AE – Autoencoder; RFE – Recursive feature elimination; PCA – Principal component analysis

Table 5: Experiment results for proposed method

Methods	Accuracy	Precision	Recall	F1-score
FCM	93.71±0.72	92.79±0.59	94.70±0.53	93.62±0.0.06
MLP	91.42±0.35	90.23±1.02	92.94±1.014	91.30±0.24
SVM	92.57±0.24	91.78±1.015	93.52±0.62	92.35±0.19
KNN	90.28±0.86	88.40±0.95	92.35±0.93	90.22±0.38

KNN – k-nearest neighbors; SVM – Support vector machine; MLP – Multilayer perceptron; FCM – Fuzzy cognitive maps

Table 6: Performance comparison of support vector machine kernels

Kernel	Accuracy (%)
Linear	85.42±1.02
Polynomial	88.74±0.91
Gaussian (proposed)	92.57±0.86

To further evaluate the impact of kernel selection in classification performance, we compared different SVM kernels under the same experimental conditions in Table 6. Table 6 provides further insights into the impact of kernel selection on SVM performance. The Gaussian kernel, which was used in the proposed method, outperformed both the linear and polynomial kernels, achieving an accuracy of 92.57%. The linear kernel (85.42%) and polynomial kernel (88.74%) showed progressively lower accuracies, suggesting that the Gaussian kernel is better suited to handle the nonlinear relationships in the data, which is likely a characteristic of multimodal medical data.

The results of the proposed method for AD diagnosis highlight several key contributions and demonstrate the effectiveness of the approach. This study introduces three major novelties: (1) the fusion of multimodal features from MRI and PET data, (2) the use of an AE model with a specified number of layers for feature reduction, and (3) the application of the CM method for classification.

Table 7 presents a comparative analysis of recent studies utilizing various methodologies for neuroimaging-based classification. Desai *et al*.[38] employed a CNN-based deep learning (DL) approach with MRI and PET fusion on the ADNI dataset, achieving 90% accuracy. Dolci *et al*.[39] utilized multimodal MRI for amyloid detection in an unbalanced cohort, obtaining 76.2% accuracy. Wang *et al*.[40] applied deep joint learning with MRI and genetic data on the ADNI dataset, reaching 93.4% accuracy. Another study[19] leveraged a fuzzy inference system with statistical features from 116 ROIs in the ADNI dataset, yielding 86.22% accuracy. The proposed method in this study introduces a novel CAD system that integrates structural MRI (sMRI) and PET using fuzzy cognitive maps (FCM) and an AE-based feature fusion approach, achieving the highest accuracy of 93.71% on the ADNI dataset. Additionally, while Reference[19] applied a rule-based fuzzy inference system, our study utilizes FCM, which provides enhanced adaptability by handling uncertainty and overlapping class distributions in neuroimaging data. These methodological improvements result in a higher classification accuracy of 93.71%, compared to 86.22% in reference[19] demonstrating the advantage of AE-driven feature extraction and FCM-based classification over traditional statistical feature selection and rule-based inference.

Figure 5a presents the confusion matrix for the FCM classifier, which achieved the highest accuracy compared to other classification methods. The FCM algorithm effectively combines fuzzy theory and neural networks, enabling it to handle the complexity and uncertainty inherent in neuroimaging data. This adaptability likely contributed to its superior performance in distinguishing between AD and

Table 7: Summarized table: Multimodal approaches for Alzheimer's disease diagnosis

Study	Methodology	Dataset	Accuracy (%)
[38]	CNN-based deep learning with MRI and PET fusion	ADNI	90
[39]	Multimodal MRI for amyloid detection	Unbalanced cohort	76.2
[40]	Deep joint learning with MRI and genetic data	ADNI	93.4
[19]	Fuzzy inference system with statistical features from 116 ROIs	ADNI	86.22
The proposed method	Novel CAD system integrating sMRI and PET using FCM and AE-based feature fusion	ADNI	93.71

CAD – Computer-aided diagnosis; CNN – Convolutional neural networks; sMRI – Structural magnetic resonance imaging; PET – Positron emission tomography; ADNI – Alzheimer's disease neuroimaging initiative; AE – Autoencoder; ROIs – Regions of interests; FCM – Fuzzy cognitive maps

HC subjects. For comparison, Figure 5b shows the confusion matrix for the MLP classifier. The MLP method performed well but achieved lower accuracy than FCM due to its simpler architecture and lack of fuzzy logic capabilities. Similarly, the SVM classifier, shown in Figure 5c, demonstrated better performance than MLP and KNN. SVM is known for its effectiveness in handling high-dimensional data; however, it still fell short of the FCM method's accuracy. Finally, the confusion matrix for the KNN classifier is presented in Figure 5d. KNN exhibited the weakest performance among the classifiers, reflecting its limitations in managing complex, high-dimensional datasets compared to FCM and SVM.

Discussion

AD continues to be a major concern as it affects a large number of elderly individuals, and its prevalence is rising globally. Early and accurate diagnosis of AD is crucial for timely intervention and treatment, which has driven significant advancements in diagnostic methods. While clinical approaches such as the MMSE and Mini-Cog Test have long been used, these methods are often limited by their subjectivity and inability to provide detailed information about the underlying brain changes associated with AD. Neuroimaging techniques, particularly sMRI and PET, have become increasingly important in AD diagnosis, as they offer noninvasive ways to visualize brain abnormalities related to the disease. Despite their effectiveness, interpreting sMRI and PET data presents challenges due to the complexity and high dimensionality of these modalities. To address these challenges, the application of AI and ML techniques has become a focus of recent research to assist clinicians in diagnosing AD more accurately and efficiently.

This study proposed a novel ML-based method for diagnosing AD by combining sMRI and PET data. The ADNI dataset,[21] which includes data from both AD patients and HC, was used to develop and evaluate the method. The preprocessing of sMRI and PET images was performed using the FSL and SPM toolboxes, respectively. Feature extraction was performed on both sMRI and PET images, yielding 108 features from the sMRI data and 27 features from the PET data per subject. One of the key innovations of this study was the fusion of these features from both modalities, which allowed for a more comprehensive representation of the brain's structure and function. The fusion of sMRI and PET features is the first novelty of this work, as it helps capture both anatomical and functional aspects of brain abnormalities that are crucial for AD diagnosis.

Another important innovation was the use of an AE model for dimensionality reduction. The AE model, with a proposed number of layers, was used to reduce the extracted features, preserving essential information while reducing the dimensionality of the feature set. This step significantly improved the computational efficiency and accuracy of the classification process. The final classification was performed using four different ML algorithms: FCM,[34] SVM,[35] KNN,[36] and MLP.[37] Among these, the FCM method achieved the highest accuracy, showcasing the potential of fuzzy logic-based models combined with neural networks in handling the complexity of multimodal neuroimaging data.

The performance variations among classifiers can be attributed to differences in how each model handles high-dimensional, complex neuroimaging data. SVM performed well but was limited in its ability to capture intricate, nonlinear relationships within the multimodal feature space, particularly due to kernel limitations in mapping highly diverse feature sets. KNN struggled with high-dimensional data, where the curse of dimensionality significantly affected its ability to compute meaningful distances between samples, leading to suboptimal classification performance. MLP, while powerful, requires extensive training data to generalize well; given our dataset size, it was prone to overfitting, resulting in reduced generalization capability.

FCM, on the other hand, effectively combines fuzzy logic with cognitive mapping, allowing it to model complex relationships between features while handling uncertainty and overlapping class distributions more effectively. This advantage enables FCM to integrate both structural and functional biomarkers in a more interpretable manner.

The results show that the proposed method outperforms other approaches in terms of accuracy, with an impressive accuracy

rate of 93.71%. This improvement in performance highlights the effectiveness of integrating sMRI and PET data, applying AE-based feature reduction, and using FCM for classification.

The comparative analysis of AE, PCA, and RFE demonstrated that AE provided better feature selection for neuroimaging data by preserving intricate nonlinear structures while reducing dimensionality. Although PCA is commonly used for dimensionality reduction, its linear nature limited its ability to capture complex patterns in MRI-PET data. RFE performed well but was computationally expensive, making it less practical for large-scale neuroimaging studies. The AE-based approach led to improved classification accuracy by maintaining essential feature representations and mitigating redundancy. These findings support the use of AE as an effective feature selection method for multimodal AD diagnosis and highlight its advantages over conventional techniques.

The superior performance of the proposed method suggests its potential for integration into clinical settings, where it could aid clinicians in diagnosing AD more quickly and accurately, potentially leading to earlier interventions.

While this study demonstrated the effectiveness of combining AI techniques with neuroimaging modalities, there are still several avenues for improvement. One promising direction is the use of DL models for AD diagnosis, as they have shown great potential in processing complex multimodal data. Future research could explore hybrid models that combine traditional ML techniques with DL models for even greater diagnostic accuracy. These models could be used to extract nonlinear features from raw sMRI and PET data, followed by fusion of manual and DL-extracted features for classification. Another exciting avenue for future work is the application of DL-based graph models, which have been shown to be effective in analyzing complex relationships between different brain regions and could provide new insights into AD diagnosis from sMRI and PET images. These advancements could further enhance the diagnostic capabilities of AI-powered systems and improve the early detection and management of AD.

In conclusion, this study presents a promising approach for AD diagnosis that combines the strengths of multimodal neuroimaging, ML, and feature fusion. The use of an AE for dimensionality reduction and the application of FCM for classification represents a significant advancement in the field. The proposed method shows great potential for use in clinical settings, providing a reliable tool to assist in the diagnosis of AD.

In the proposed method, an AE was used for feature reduction, and hyperparameter tuning was performed without extensive cross-validation due to computational constraints. Additionally, the computational complexity of the proposed approach, particularly in feature extraction and AE-based dimensionality reduction, may pose challenges for real-time clinical application. While trial-and-error tuning provided effective results given the dataset size and computational constraints, we acknowledge that more systematic approaches, such as grid search or cross-validation, could further optimize parameter selection.

Future work should address these limitations by incorporating larger and more diverse datasets, performing external validation, and optimizing computational efficiency. Future work, including the integration of DL techniques and graph-based models, holds the promise of further improving the accuracy and applicability of AD diagnostic systems.

Conclusions

This study introduced a novel ML-based approach for the diagnosis of AD using multimodal MRI and PET data. The preprocessing of sMRI and PET data was performed using the FSL and SPM toolboxes, respectively, ensuring high-quality data for the analysis. Feature extraction techniques were applied to both modalities, generating a comprehensive set of structural and functional features. These features were then fused, marking the first key novelty of this research. To address the high dimensionality of the feature set, an AE model with a custom layer structure was employed for feature reduction, representing the second significant novelty. The reduced feature set was classified using various algorithms and the FCM method demonstrated the highest performance, achieving superior accuracy compared to other classifiers, highlighting the third major novelty of this study.

The results indicate that the fusion of multimodal features, AE-based feature reduction, and the FCM classification technique collectively enhance the accuracy and robustness of AD diagnosis. The proposed method outperformed existing approaches and shows great potential for the implementation in the clinical settings to aid neurologists in the early and accurate detection of AD.

Supplementary materials

Table 8 presents various extracted image features and their relevance to AD diagnosis. It categorizes the features based on different texture analysis methods, including the GLCM, GLHA, NGTDM, and GLSZM. GLCM features such as energy, contrast, correlation, and entropy assess structural consistency, intensity variation, neurodegenerative patterns, and randomness in brain images. GLHA features, including mean intensity and variance, help to detect changes in GM density and tissue degeneration. NGTDM features such as busyness and coarseness analyze local and spatial intensity variations, aiding in functional assessment. Finally, GLSZM features such as small area emphasis and zone percentage focus on fine-grain textural changes and large-scale neurodegenerative patterns, making them crucial for identifying disease progression. These features collectively

Table 8: Extracted features and their relevance to Alzheimer's disease diagnosis

Feature type	Feature name	Description	Relevance to AD diagnosis
GLCM	Energy	Measures textural uniformity	Detects structural consistency in brain regions
	Contrast	Measures intensity variation	Highlights cortical atrophy and tissue degradation
	Correlation	Measures pixel relationship	Identifies the patterns of neurodegeneration
	Entropy	Measures randomness	Indicates disorganization in brain structures
GLHA	Mean intensity	Average pixel intensity	Detects changes in gray matter density
	Variance	Intensity spread measure	Highlights tissue degeneration
NGTDM	Busyness	Measures local intensity variation	Identifies functional irregularities in PET
	Coarseness	Measures spatial intensity variation	Helps in tissue differentiation
GLSZM	Small area emphasis	Measures distribution of small homogeneous zones	Highlights fine-grain textural changes
	Zone percentage	Measures the uniformity of zones	Detects large-scale neurodegenerative patterns

AD – Alzheimer's disease; GLCM – Gray level co-occurrence matrix; GLSZM – Gray level size zone matrix; NGTDM – Neighborhood gray tone difference matrix; GLHA – Gray level histogram analysis; PET – Positron emission tomography

enhance the accuracy of AD diagnosis by capturing structural and functional abnormalities in brain imaging.

Ethical approval

The data used in this study were obtained from the publicly available Alzheimer's Disease Neuroimaging Initiative (ADNI) dataset. Ethical approval and participant consent were obtained by the ADNI investigators, and all procedures were conducted in accordance with relevant guidelines and regulations.

Funding

This research did not receive any specific grant funding.

Availability of data and materials

The data utilized in this study are publicly available from the ADNI database.

Financial support and sponsorship

Nil.

Conflicts of interest

The authors declare that they have no conflict of interest.

References

1. Weller J, Budson A. Current understanding of Alzheimer's disease diagnosis and treatment. F1000Res 2018;7:v1000-161.
2. Khachaturian ZS. Diagnosis of Alzheimer's disease. Arch Neurol 1985;42:1097-105.
3. Dubois B, Villain N, Frisoni GB, Rabinovici GD, Sabbagh M, Cappa S, *et al.* Clinical diagnosis of Alzheimer's disease: Recommendations of the International Working Group. Lancet Neurol 2021;20:484-96.
4. Brazaca LC, Sampaio I, Zucolotto V, Janegitz BC. Applications of biosensors in Alzheimer's disease diagnosis. Talanta 2020;210:120644.
5. Arevalo-Rodriguez I, Smailagic N, Roqué I Figuls M, Ciapponi A, Sanchez-Perez E, Giannakou A, *et al.* Mini-Mental State Examination (MMSE) for the detection of Alzheimer's disease and other dementias in people with mild cognitive impairment (MCI). Cochrane Database Syst Rev 2015;2015:CD010783.
6. Fage BA, Chan CC, Gill SS, Noel-Storr AH, Herrmann N, Smailagic N, *et al*. Mini-Cog for the diagnosis of Alzheimer's disease dementia and other dementias within a community setting. Cochrane Database Syst Rev 2015. p. CD010860.
7. Li F, Liu M, Alzheimer's Disease Neuroimaging Initiative. Alzheimer's disease diagnosis based on multiple cluster dense convolutional networks. Comput Med Imaging Graph 2018;70:101-10.
8. Cui R, Liu M. Hippocampus analysis by combination of 3-D DenseNet and shapes for Alzheimer's disease diagnosis. IEEE J Biomed Health Inform 2019;23:2099-107.
9. Burton EJ, Barber R, Mukaetova-Ladinska EB, Robson J, Perry RH, Jaros E, *et al.* Medial temporal lobe atrophy on MRI differentiates Alzheimer's disease from dementia with Lewy bodies and vascular cognitive impairment: A prospective study with pathological verification of diagnosis. Brain 2009;132:195-203.
10. Veitch DP, Weiner MW, Aisen PS, Beckett LA, Cairns NJ, Green RC, *et al.* Understanding disease progression and improving Alzheimer's disease clinical trials: Recent highlights from the Alzheimer's disease neuroimaging initiative. Alzheimers Dement 2019;15:106-52.
11. Dimitriadis SI, Liparas D, Alzheimer's Disease Neuroimaging Initiative. How random is the random forest? Random forest algorithm on the service of structural imaging biomarkers for Alzheimer's disease: From Alzheimer's disease neuroimaging initiative (ADNI) database. Neural Regen Res 2018;13:962-70.
12. Whitwell JL. Alzheimer's disease neuroimaging. Curr Opin Neurol 2018;31:396-404.
13. Frisoni GB, Fox NC, Jack CR Jr., Scheltens P, Thompson PM. The clinical use of structural MRI in Alzheimer disease. Nat Rev Neurol 2010;6:67-77.
14. Chételat G, Arbizu J, Barthel H, Garibotto V, Law I, Morbelli S, *et al.* Amyloid-PET and (18) F-FDG-PET in the diagnostic investigation of Alzheimer's disease and other dementias. Lancet Neurol 2020;19:951-62.
15. Shoeibi A, Khodatars M, Jafari M, Moridian P, Rezaei M, Alizadehsani R, *et al.* Applications of deep learning techniques for automated multiple sclerosis detection using magnetic resonance imaging: A review. Comput Biol Med 2021;136:104697.
16. Polikar R, Tilley C, Hillis B, Clark CM. Multimodal EEG, MRI and PET data fusion for Alzheimer's disease diagnosis. Annu Int Conf IEEE Eng Med Biol Soc 2010;2010:6058-61.
17. Tabarestani S, Aghili M, Shojaie M, Freytes C, Adjouadi M. Profile-specific regression model for progression prediction of

Alzheimer's disease using longitudinal data. In 2018 17th IEEE International Conference on Machine Learning and Applications (ICMLA) 2018. p. 1353-7.
18. Ding J, Huang Q. Prediction of MCI to AD conversion using Laplace Eigenmaps learned from FDG and MRI images of AD patients and healthy controls. 2017 2nd International Conference on Image, Vision and Computing (ICIVC), 2017. p. 660-4.
19. Krashenyi I, Ramírez J, Popov A, Górriz JM, The Alzheimer's Disease Neuroimaging Initiative. Fuzzy computer-aided Alzheimer's disease diagnosis based on MRI data. Curr Alzheimer Res 2016;13:545-56.
20. Akhila D, *et al*. Robust Alzheimer's Disease Classification Based on Multimodal Neuroimaging. 2016 IEEE International Conference on Engineering and Technology (ICETECH); 2016. p. 748-52.
21. Forouzannezhad P, Abbaspour A, Cabrerizo M, Adjouadi M. Early diagnosis of mild cognitive impairment using random forest feature selection. In 2018 IEEE Biomedical Circuits and Systems Conference (BioCAS); 2018. p. 1-4.
22. Sheng J, Zhang Q, Zhang Q, Wang L, Yang Z, Xin Y, *et al*. A hybrid multimodal machine learning model for detecting Alzheimer's disease. Comput Biol Med 2024;170:108035.
23. Tang Y, Xiong X, Tong G, Yang Y, Zhang H. Multimodal diagnosis model of Alzheimer's disease based on improved transformer. Biomed Eng Online 2024;23:8.
24. Castellano G, Esposito A, Lella E, Montanaro G, Vessio G. Automated detection of Alzheimer's disease: A multi-modal approach with 3D MRI and amyloid PET. Sci Rep 2024;14:5210.
25. Choudhury C, Goel T, Tanveer M. A coupled-GAN architecture to fuse MRI and PET image features for multi-stage classification of Alzheimer's disease. Inf Fusion 2024;109:102415.
26. Zhang Y, He X, Chan YH, Teng Q, Rajapakse JC. Multi-modal graph neural network for early diagnosis of Alzheimer's disease from sMRI and PET scans. Comput Biol Med 2023;164:107328.
27. Dukart J, Mueller K, Barthel H, Villringer A, Sabri O, Schroeter ML, *et al.* Meta-analysis based SVM classification enables accurate detection of Alzheimer's disease across different clinical centers using FDG-PET and MRI. Psychiatry Res 2013;212:230-6.
28. Lazli L, Boukadoum M, Ait Mohamed O. Computer-aided diagnosis system of Alzheimer's disease based on multimodal fusion: Tissue quantification based on the hybrid fuzzy-genetic-possibilistic model and discriminative classification based on the SVDD model. Brain Sci 2019;9:289.
29. Zhou Q, Goryawala M, Cabrerizo M, Barker W, Loewenstein D, Duara R, *et al.* Multivariate analysis of structural MRI and PET (FDG and 18F-AV-45) for Alzheimer's disease and its prodromal stages. Annu Int Conf IEEE Eng Med Biol Soc 2014;2014:1051-4.
30. Ferreira LK, Rondina JM, Kubo R, Ono CR, Leite CC, Smid J, *et al.* Support vector machine-based classification of neuroimages in Alzheimer's disease: Direct comparison of FDG-PET, rCBF-SPECT and MRI data acquired from the same individuals. Braz J Psychiatry 2018;40:181-91.
31. Alongi P, Sardina DS, Coppola R, Scalisi S, Puglisi V, Arnone A, *et al.* 18F-florbetaben PET/CT to assess Alzheimer's disease: A new analysis method for regional amyloid quantification. J Neuroimaging 2019;29:383-93.
32. Ortiz A, Munilla J, Álvarez-Illán I, Górriz JM, Ramírez J, Alzheimer's Disease Neuroimaging Initiative. Exploratory graphical models of functional and structural connectivity patterns for Alzheimer's disease diagnosis. Front Comput Neurosci 2015;9:132.
33. Zabalza J, Ren J, Zheng J, Zhao H, Qing C, Yang Z, *et al*. Novel segmented stacked autoencoder for effective dimensionality reduction and feature extraction in hyperspectral imaging. Neurocomputing 2016;185:1-10.
34. Gonzalo N, Espinosa M, Grau I, Vanhoof K, Bello R. Fuzzy cognitive maps based models for pattern classification: Advances and challenges. Soft Computing Based Optimization and Decision Models: To Commemorate the 65th Birthday of Professor José Luis" Curro" Verdegay 2017. p. 83-98.
35. Noble WS. What is a support vector machine? Nat Biotechnol 2006;24:1565-7.
36. Taunk K, De S, Verma S, Swetapadma A. A brief review of nearest neighbor algorithm for learning and classification. In 2019 international conference on intelligent computing and control systems (ICCS); 2019:1255-60.
37. Zanaty EA. Support Vector Machines (SVMs) versus Multilayer Perception (MLP) in data classification. Egypt Inform J 2012;13:177-83.
38. Desai MB, Kumar Y, Pandey S. Efficient Approach for Diagnosis and Detection of Alzheimer Diseases Using Deep Learning. In 2024 International Conference on Advances in Computing Research on Science Engineering and Technology (ACROSET). 2024; IEEE.
39. Dolci G, Ellis CA, Cruciani F, Brusini L, Abrol A, Galazzo IB, *et al.* Multimodal MRI accurately identifies amyloid status in unbalanced cohorts in Alzheimer's disease continuum. Netw Neurosci 2025;9:259-79.
40. Wang J, Wen S, Liu W, Meng X, Jiao Z. Deep joint learning diagnosis of Alzheimer's disease based on multimodal feature fusion. BioData Min 2024;17:48.